Study of aero-engine oil/air separators

C N Eastwick[1], K Simmons[1], Y Wang[2] & S Hibberd[1]

1 University Technology Centre in Gas Turbine Transmission Systems (UTC), University of Nottingham, University Park, Nottingham, NG7 2RD

2 Formerly Nottingham Transmissions UTC, now at Rolls-Royce Plc., PO Box 31, Derby, DE24 8BJ

Abstract

For aero-engines, oil/air separation is a key function and one approach to assessing separator effectiveness is computational fluid dynamics (CFD). The two-phase flow is complex and oil can be present in different forms (for example droplets, mist, film). However, necessary modelling simplifications may affect solution accuracy and range of validity. This paper presents a modelling methodology for oil/air separators; the effect of simplifications is discussed and their relative magnitude assessed. Comparison with available experimental data is presented. It is concluded that whilst simplification has an impact, the significant features of the oil-air separator are predicted with sufficient accuracy to allow design comparisons.

Two separator configurations, one internal to a bearing chamber and one external, are modelled and the data presented. Flow fields are compared and the effectiveness of the separators at removing oil droplets prior to impact on the breather (primary separation) presented. The separation performance of the external design is largely independent of shaft speed with all droplets greater than 3µm removed before impact on the breather. The critical droplet diameter of the internal design is larger, varying

with breather configuration and shaft speed but the power loss is an order of magnitude lower than for the external design.

Keywords: CFD; Two Phase Flow, Oil/air Separator; Gas Turbine; Breather; Aero-engine

Notation

Symbol	Quantity	Unit
W_L	Power loss	W
$\dot{m}$	Mass flow rate	kg/s
g	Gravitational acceleration	kgm/s^2
H_L	Total Head Loss	m

1. Introduction

Within the transmission system of a gas turbine aero-engine the lubrication and cooling of shaft bearings is performed by oil injected into sealed bearing chambers. The subsequent oil-air mixture is recovered and separated such that the oil is re-used and the air is discharged overboard. Separation efficiency (percentage of oil recovered from the separator) is a high priority, with any loss of oil an environmental concern. An aim of the work described here is to provide a methodology for the comparison of different designs of oil-air separators, to allow greater understanding of separator behavior and to facilitate the improvement of current designs.

An aero-engine oil-air separator typically consists of a stationary chamber containing a rapidly rotating hollow shaft. A porous metal (or plastic) matrix in a housing is rigidly mounted on the shaft such that shaft, porous media and housing all rotate together; the porous media and its housing are commonly referred to as a *breather*. As the oil/air mixture enters the chamber some of the oil is centrifuged to the chamber walls where it forms a film that travels to a scavenge (exit) point. Smaller oil droplets and the air pass into the porous media where the air continues through to the shaft centre and is vented to atmosphere. In the porous media small oil droplets coalesce and are transported to the outside of the breather where they are flung out to the walls. The separation of oil from the oil-air mixture is therefore achieved partially by the centrifuging of larger oil droplets (primary separation) and partly by the coalescence and centrifuging of oil in the porous matrix (secondary separation).

Within the European aero-engine industry there are two prevalent configurations, an *internal* design where the breather is housed inside a bearing chamber and an *external* design where the scavenged flows from bearing chambers are ducted to an external separator. In this paper data from CFD models of internal and external separator designs are investigated and compared. In addition, available experimental data for the internal design is compared to the CFD model.

2. Previous Work

Very little work directly relevant to the oil-air separation process within a rapidly rotating flow has been carried out as both experimental work and numerical modelling have attendant difficulties. The University of Nottingham Technology Centre in Gas Turbine Transmissions has conducted related research into droplet and film flows in

aero-engine bearing chambers. The group has applied commercial CFD codes **[1, 2]** modelling single phase air flow and applying Lagrangrian droplet tracking as a preliminary approach to multiphase modelling. An in-house code for thin film modelling **[3, 4]** has been developed and successfully applied to an industrial bearing chamber design. An amount of preliminary research into oil/air separators carried out at Nottingham under Brite Euram project INTRANS has also been published **[5, 6]** although some work relevant to oil-air separation is not yet in the open literature **[7]**.

Related work has also been undertaken by the Institute of Thermal Turbomachinery at the University of Karlsruhe, where aero-engine bearing chamber flow has been studied. Wittig et al **[8, 9]** reported an experimental investigation into oil film thickness and heat transfer in aero-engine bearing chambers under the influence of high rotational speeds up to 16000 rpm. In following work **[10, 11]** measurements of oil film velocity profiles in a high speed bearing chamber rig simulating engine conditions were carried out and the results were compared with theoretical predictions.

3. Developing an appropriate CFD approach

Within separators/bearing chambers oil can be present as droplets, films and mist (sub-micron droplets). There are a number of physical processes taking place including draining films passing into pipe-work, droplet impact onto films and generation of droplets from films. Although each of these phenomena may be computed separately, investigating all the interactions simultaneously is still beyond the capabilities of realistic CFD, especially within a commercially acceptable

computing time. It is evident that some simplification is required and in this section potential simplifications and assumptions are discussed.

In general, when creating a CFD model a clear formulation of the problem will identify those physical phenomena of most direct relevance. In this particular situation the interest is in assessing the effectiveness of separator designs in removing oil from the air before it is vented. As mentioned in the introduction, oil removal is a two stage process consisting of primary separation in the chamber and secondary separation in the porous breather. This paper concentrates on the effectiveness of primary separation; seeking to establish what, if any, limits exist to total oil/air separation in the chamber and how close the chosen designs come to that limit.

3.1 Simplifications and Assumptions

There are three distinct reasons for incorporating simplifications or assumptions: coding constraints (physical situation cannot be fully modelled by code), unknown physics (boundary or inlet conditions not fully known) and time constraints (aimed at reducing computing time).

(i) Simplifications due to coding constraints

In this study a Lagrangian approach to modelling the oil phase was adopted. Tracking the oil droplets through the porous media is beyond the capability of the CFD code and would in any case require detailed knowledge of the exact form of the porous material itself. Consequently oil tracking is terminated at the porous face. The impact on the calculation is that droplets created by coalescence within the breather and ejected into the main chamber are not included. The volume of oil being spun out

from the breather is small (volume fraction of 2 - 7% at operating speeds) and consists of small diameter droplets (15 - 25 μm). Consequently it is not judged to constitute a large enough fraction of the oil flow to transfer significant momentum to the air flow. Therefore the simplification has a negligible affect on the area of interest within the calculation. There would be an effect on any films running around the walls of the separator chamber; however these are not being modelled (see simplifications due to physical unknowns).

Due to code constraints the porous media is modelled as stationary, where in reality it rotates with the shaft and holder. This simplification will affect flow around the face region since in reality the face will act as a rotating disk, imparting angular motion to the fluid as illustrated by the experiments by Daily & Nece **[12]**. Rotation of the porous media would provide a radially outward force on the fluid, causing a maximum increase in velocity of 0.6m/s for a shaft rotational speed of 5000 rpm. In the computed flow field the radial velocity is small (4 m/s at 5,000 rpm) compared to the azimuthal velocity (of order 100 m/s). It is not felt that this necessary simplification will significantly affect the outcome of the calculations.

The oil droplets are modelled as spherical, droplet/droplet interactions are not included and droplets terminate once they hit a solid/porous face (no rebound or splashback). Given the nature of the droplets the assumption of sphericity is valid **[13]**. The modelling simplification that the droplets terminate at a surface may not be valid, dependent on the angle and speed of the droplet. In reality the surfaces are likely to be covered by a thin moving film **[10]**, and on impact a droplet may splash or rebound. In his model for film flow in an aero-engine bearing chamber Farrall **[14,**

15] identified four outcomes of droplet film interaction (stick, rebound, spread, and splash) dependent on the value of an impact parameter K. Although future work could include the effect of droplet/film interaction, in this study it is omitted.

(ii) Simplifications and assumptions due to physical unknowns

The mass of oil entering the chamber is known, but its format (droplets/film) and critical dimensions (diameter/shape factor) are not. A decision was made to model the oil as droplets as this allowed a Lagrangian approach to be used. A range of droplet diameters were investigated using diameters suggested by previous experimental studies **[8-11]**. Droplet release location and velocity were also not known exactly although clearly the region is identified by the location of the bearing. Consequently a realistic range of release positions was investigated.

The porous media is modelled as an isotropic porous medium of uniform construction that follows Darcy's law **[16]** (for a given material velocity is proportional to pressure gradient) as this appeared to be the best approximation based on data available at the time **[19]**. Work completed at Nottingham subsequently has suggested the Forchheimer model (pressure gradient is given by a quadratic function of velocity) would be more appropriate **[18]**. It is difficult to assess the magnitude of any uncertainty/error due to this simplification. However as the area of interest for this study is the behaviour of oil droplets in the air flow prior to entry to the porous media it is anticipated that the effect of the approximation will not be significant, affecting only the axial velocity close to the breather and pressure gradient within the porous media itself.

It is likely that oil films on chamber surfaces are thin **[10]** and in this study the model is simplified by the omission of surface films. This simplification would have a negligible effect on the air flow in terms of geometry variation. The wall boundary condition could be modified from a stationary wall to a moving wall to account for film velocity although as it is likely the film is moving slowly **[10]** this was not done in the present study.

(iii) Simplifications applied to reduce computing time

Turbulent dispersion of droplets is not included in the calculation to reduce computing time, although a sensitivity study was carried out initially to assess the validity of this simplification with regard to droplet deposition pattern.

Whilst within a gas turbine assuming isothermal conditions would not be valid, in this work comparisons are made with experimental rig data where there is little temperature variation and therefore all cases are computed isothermally.

Cases are computed as two dimensional axi-symmetric with the oil drain omitted as this simplification significantly reduces computing time. The geometry is largely axi-symmetric with the exception of the oil drain so some local variation between model and reality would be expected in that region. The oil phase was computed in such a manner that the associated mass is removed from the calculation without the need for an oil drain.

4 Separator designs

Two oil/air separator designs are investigated in this paper, one is an internal design, where the separator is housed within a bearing chamber and the second an external design, which is housed in a separate chamber. Both designs are simplifications of existing commercial separators.

4.1 Internal oil-air separator

A two dimensional schematic drawing of an internal oil-air separator is shown in Figure 1. Two oil-lubricated bearings (front and rear) support a hollow highly rotating shaft. A breather consisting of a cylindrical housing containing blocks of Retimet (a patented porous metal matrix **[17]**).is mounted on the rotating shaft. The inside of the breather housing has slots that interface with holes in the shaft to allow the cleaned air to exhaust. The breather housing has three configurations depending on whether the oil/air mixture enters through the front face only, the rear face only or both (Fig 1 shows the rear-face-open configuration).

Air enters the bearing chamber through the front and rear bearings. In the CFD model the air from the front bearing is considered as divided into two paths (inlet 1 and inlet 2) with only the air of inlet 2 entraining oil droplets as it enters the chamber. Although oil and air can enter the chamber through the rear bearing, the mass flow of oil and air associated with this bearing is an order of magnitude smaller than that from the front bearing and so the rear bearing flow has not been included in the CFD model.

4.2 External Design

Figure 2 shows a sectional view of an external oil-air separator. The separator system consists of a rotating hollow shaft running in a stationary concentric cylindrical chamber with the breather mounted on the rotating shaft. The inside of the breather housing has slots that coincide with holes in the shaft to allow air to exhaust through the shaft in a similar manner to the internal oil-air separator. The external separator has two tangential air and oil inlets one is in front of the breather housing (shown in Fig 2) and the other is at the rear of the housing (not illustrated). Configurations with inlet flow from the front inlet only and both inlets are considered. As with the internal separator, primary oil/air separation takes place in the chamber as larger droplets are centrifuged to the chamber walls and secondary separation takes place inside the breather.

There are two main differences between the external and internal designs: the manner in which the oil and air are introduced to the chamber and the relative size of the chamber housing. In the internal design oil enters the chamber through the bearing (essentially axially) whereas in the external design the oil/air inlets are located so as to promote azimuthal motion within the chamber thereby enhancing primary separation. In the internal design the chamber is quite large with respect to the breather as chamber size is dictated by the bearings. In the external design the chamber has to be as small as physically possible because of engine space constraints and so there is not much clearance between chamber walls and breather housing. The breathers themselves are essentially the same although small differences exist in housing design.

5. CFD Methodology

5.1 Solution Strategy

The single-phase airflow within the separators was modeled using the commercial CFD code CFX4.2 **[20].** The air flow was modeled as steady state, turbulent, isothermal and incompressible. Oil droplet trajectories were computed using a Lagrangian tracking approach, two-way coupled to the airflow. The standard k-ε model turbulence model was applied to the airflow **[21]** and turbulent dispersion of the oil droplets was not included. The flow in the porous media was modelled using Darcy's law with the volume porosity set to 0.95 and the resistance constant taken as 6000 kg/m^{3}s, consistent with performance data supplied by the manufacturers **[19]**.

5.2 Computational Meshes

The grid employed for the internal design is 2D axisymmetric and has 13400 cells, a compromise between the time available for computations and the size of the near wall cells, which are constrained by the range of validity of the wall function in conjunction with the standard k-ε turbulence model. For the external design a full 3D model was required and this had 215,000 cells.

5.3 Boundary conditions

The velocity at the inlets is specified as uniform, and determined from the air flux and inlet area. The rotational speed of the shaft is defined by specifying tangential velocities on the wall. The walls of the breather housing are also modelled as rotating. However, the porous media within the breather is modelled as stationary due to modeling constraints (see section 3.1). For the internal separator model the centreline of the shaft is modelled as a symmetry plane (as is standard in some CFD

codes) and the bounding angular planes are modelled as periodic. A full 3D model of the external separator was created. Model specific boundary conditions are given in Table 1.

	Internal Separator	External Separator
Inlet air flux modelled	25 g/s & 50 g/s	45 g/s
Shaft speeds modelled	0 – 10,000 rpm	0 – 10,000 rpm
Typical operational speed	3000 rpm	7,500 rpm
Droplet diameters modelled	Rosin-Rammler, $\bar{d} = 100\mu m$, spread factor 2	1μm to 100μm

Table 1: Modelling boundary conditions

5.3 Discretisation scheme and solution algorithm

The hybrid scheme **[22]** is used for discretising the governing equations. The SIMPLEC solution algorithm **[23]** is used to provide the pressure-velocity coupling in the outer iteration. The discretised equation for each variable is solved by the Algebraic Multi Grid method **[24]** in the inner iteration.

6. Validation Data

There is only validation data available for the internal separator design at one configuration (rear face open) and full details of the experimental tests can be found in Aroussi & Menacer **[7]**. On the test rig the outer chamber of the separator was replaced by a casing with a number of windows allowing optical access. A non-intrusive optical anemometer was used to acquire data on the velocity, size and

concentration of oil droplets. Measurements were taken on a series of two-dimensional planes within the bearing chamber, for three shaft speeds 1100 rpm, 3000 rpm and 5000 rpm. Unfortunately a number of difficulties were encountered during the experimental tests and these restricted access such that there is uncertainty in the exact location of the measurement planes. The planes were positioned by eye, with measurements taken over several days. Particle tracking software was used to generate droplet velocity data and this is compared to CFD airflow data. Experimentally a range of droplet diameters were encountered, but only the smaller droplets (Stokes Number significantly less than 1) will follow the air flow. To account for the uncertainty in plane location and the effect of larger oil drops on the data, uncertainty bars of ±30% have been added to the experimental data. It is anticipated that this compound uncertainty provides a conservative estimate. Comparisons are available for one plane, shown on Figure 1.

7. Results

7.1 Internal design

Three breather configurations were considered and the air flow fields at 1100 rpm and 5000 rpm for each configuration are shown in Figure 3. Comparing the flows at 1100 rpm and 5000 rpm for all three configurations increasing the rotational speed leads to a stronger and radially wider recirculation to the left of the breather housing and a stronger recirculation to the right of the breather housing. It can be seen that the front open configuration sets up the strongest outward flow at higher speeds from the rotating back of the breather housing, causing any larger droplets in this area to be flung to the outer wall. However, the front open configuration has the most direct path from inlet to porous media and would therefore be most likely to take droplets

straight to breather. The rear open configuration has the most tortuous path to the open face of the porous media with strong flows to the end wall of the chamber, so it would be expected that this design would be the most effective at preventing droplets impacting the breather. The front-and-rear configuration exhibits a similar flow pattern to the rear open configuration, although not surprisingly the rear open configuration has a stronger axial flow over the top of the breather housing.

Figure 4 shows droplet trajectories for the best and worst primary separation cases. For the front open case at low shaft speed (Fig 4a) it can be seen that the majority of the droplets impinge on the breather with only the largest droplets travelling undeflected to the rear of the chamber. With the rear-open case at 5,000 rpm (Fig 4b) only the smallest droplets impinge on the breather and primary separation is significantly enhanced.

Comparison to experimental data

Figures 5 compares velocity profiles for the front-open configurations at 1100 rpm and 5000 rpm on the plane identified in Figure 1 with experimental data. The x-axis shows non-dimensional radial distance from breather housing with 0 corresponding to shaft outer diameter and 1 corresponding to chamber wall. In both cases the trend is well-predicted with the magnitude less so, particularly away from the shaft.

Figures 6 shows CFD to experimental data comparisons for the rear open configuration at 1100 rpm and 3000 rpm. At 1100 rpm the trend prediction is reasonable although the velocity magnitude is significantly under-predicted by the CFD. At 3000 rpm there is significant difference in the trends predicted although the

velocity magnitudes are adequate. Given the significant uncertainties associated with the experimental data, the validation obtained might be regarded as adequate although ideally further work would be required.

7.2 External Design

Calculations were carried out for shaft speeds in the range 0 – 10,000 rpm for two configurations, one with all the flux entering through the front inlet and the second with the flux split evenly between the two. In both cases the inlet flow, combined with the small chamber size, creates a highly swirling flow. The curvature of the air streamlines is significant such that only small droplets impinge on the breather at all. With two inlets the flow is more even along the length of the separator but the main effect can be seen on the droplet trajectories. Figures 7a) and b) show trajectories of droplets released from inlet 1 for single inlet (a) and dual inlet (b).

Although droplets in the range 1μm to 100μm were investigated, those greater than 4μm are barely deflected on entry and travel to the chamber wall opposite the inlet. Figure 7 shows that the smaller droplets entering the chamber do not travel as far axially when the second inlet is included.

7.3 Parameters of comparison

In order to assess and compare the effectiveness of the two designs at removing oil from the air prior to entry into the breather, two parameters of comparison were chosen. These are the separator power loss ($W_L = \dot{m}gH_L$) and the critical droplet diameter. The dependency of both parameters on shaft speed is assessed. The critical droplet diameter is the size of the smallest droplet impinging on the breather and is

therefore a measure of primary separation effectiveness. Power loss is important as all parasitic losses in aero-engines have an associated cost although only some of the loss in the internal separator design is directly associated with the separation process. Separation efficiency (percentage of oil recovered from the separator) is a function of primary and secondary separation effectiveness and these in turn depend on the form of the oil at entry to the separator and the size distribution of oil droplets present. The critical droplet diameter is therefore only one of the significant pieces of information required in assessing overall separation efficiency.

There is a significant difference in power loss behaviour in the two designs. Figure 8a) shows that for the internal design power loss increases quadratically with shaft speed. A second order polynomial trendline fitted to the rear-open data is almost indistinguishable from the data line. There is some variation in the three breather configurations with the rear-open case giving lower losses at low speed and higher losses at higher speeds compared to the front-open case. For the external design the power loss varies very little with shaft speed, but compared to the internal design the loss is high for all speeds. At 10,000 rpm the power loss associated with the internal design is approximately 104 W (air mass flowrate 50 g/s) compared to around 1390 W for the external design (air mass flowrate 45 g/s).

In terms of critical droplet diameter, the external separator design showed a critical droplet diameter of 3μm for the single inlet case and 4μm for the two inlet case over all speeds in the range 0 – 10,000 rpm. However the internal design showed a dependency of critical droplet diameter on both shaft speed and breather configuration as illustrated in Figure 9. For all breather configurations the critical droplet diameter

is significantly above that for the external design. The best separation is obtained with the rear open configuration at 5,000 rpm where the critical droplet diameter is 10μm.

8. Discussion

CFD has established itself as one of the primary research tools in a number of industrially-relevant research and development areas. In aero-engine separator design, as in many other cases, simplifications must be made both due to coding constraints and limitations in available data to fully define the problem. In addition, in this case simplifications were made in order to reduce computing time. One of the main advantages of CFD is that different configurations and parameter ranges can be investigated relatively easily once the validity of the initial modelling approach has been established. In this case a limited amount of experimental data was available and it compared reasonably well with the equivalent CFD data. Slight differences in CFD configuration compared to experimental configuration precluded detailed validation but nevertheless, the capability of the CFD model to capture bulk behaviour was established.

Two aero-engine oil/air separators have been investigated; the particular designs were chosen as they embody two approaches currently in use. The internal separator is integral to the bearing chamber where the oil/air mixture is created from sealing air and lubricating/cooling oil. The shaft speed is therefore limited by engine operating conditions, chamber size is determined by the bearings and oil/air inlet conditions are largely uncontrolled. The designer can alter the configuration of the breather itself and this study suggests the greater path curvature of the rear-open configuration will

improve primary separation. Compared to the external separator, power losses are far lower and are shaft speed dependent; primary separation is less effective with droplet diameters below 10μm impinging on the breather under all normal operating conditions and droplets up to 40μm impinging at lower shaft speeds.

The external separator design is optimised for oil/air separation with tangential inlets, high shaft speed and a small external chamber to enhance centrifugal separation. Oil/air mixtures from more than one source can be ducted to the separator. Primary separation for the separator investigated was very good with all droplets above 3μm removed prior to impingement on the breather at all shaft speeds. Power loss was found to be largely independent of shaft speed but around ten times higher than for the internal design.

Both designs embody a form of cyclonic separation but the external separator is most like a traditional cyclone in that the inlet flow sets up the azimuthal motion. The performance was almost unaffected by shaft rotation speed suggesting primary separation is largely independent of it. In a cyclone the pressure drop depends on the flowrate and Fig 8b suggests the external separator is behaving primarily as a cyclone with very little performance modification as a function of the rotation. In the internal separator the swirling motion is primarily set up by the shaft and breather rotation and therefore separation performance is strongly affected by shaft rotation speed.

This work suggests an external separator design may be the better choice for aero-engine applications provided the power loss "cost" is not too high. However, a number of factors have not been taken into account here. Secondary separation in the

breather as small droplets coalesce and are driven out into the chamber may be highly dependent on droplet size. In such a case secondary separation could be very effective in the internal design and largely ineffective in the external case. Anecdotal evidence suggests that submicron oil droplets will pass through the breather under all operational conditions. However, research on the effectiveness of the breather to capture oil droplets is required to assess the effects of droplet size at inlet and loading on secondary separation. A further consideration is that during primary separation larger droplets may impact on wall films sourcing smaller droplets, thereby reducing primary separation effectiveness and affecting overall separation efficiency.

9. Conclusions

A CFD methodology has been established and partially validated for evaluation of the primary separation performance of aero-engine oil-air separators. Two designs have been modeled: an internal separator and an external separator. Both rely on centrifugal separation but in the internal separator the swirling motion is created by shaft and breather rotation whereas in the external separator traditional tangential inlets set up the swirl. Primary separation was more effective in the external separator with a critical droplet diameter of only 3μm compared to 10μm in the internal design. The power loss for the external separator was calculated to be of the order of 1390 W compared to around only 104 W for the internal design; a significant difference if the overall separation performance of the internal separator is adequate.. The effectiveness of primary separation of the internal design was very shaft speed dependent whereas the performance of the external design was largely independent of shaft speed. Secondary separation remains an area of research as do the effects of droplet splashing/interaction.

Acknowledgements

The University of Nottingham Technology Centre in Gas Turbine Transmissions Systems gratefully acknowledges the financial support of the EU, Rolls-Royce Plc and Techspace Aero for this work. We would also like to acknowledge the technical support from Dunlop Equipment.

References

1. **Simmons, K., Hibberd, S., Wang, Y. & Care, I.**, "Numerical study of the two-phase air/oil flow within an Aero-Engine bearing chamber model using a coupled lagrangian droplet tracking method", 2002, PVP-Vol. 448-1, Computational Technologies for Fluid/Thermal/Structural/Chemical Systems with Industrial Applicatons, Volume 1, ASME 2002, PVP2002-1568
2. **Wang Y, Hibberd, S, Simmons, K, Eastwick, C N, and Care I**., "Application of CFD to modelling two-phase flow in a high-speed aero-engine transmission chamber", 2001 Fluids Engineering Division Summer Meeting, May 29 - June 1, 2001, New Orleans, LA.
3. **Farrall, M, Hibberd, S, Simmons, K**, "A Numerical Model For Droplet/Film Interactions In A Simplified Bearing Chamber", 2003, ICLASS 2003, Sorento, 13-18 July 2003.
4. **Farrall, M. B., Hibberd, S. and Simmons, K.,** "Computational modelling of two-phase air/oil flow within an aero-engine bearing chamber", 2000, FEDSM 2000-11081, Proceedings of ASME 2000. Fluids Engineering Division Summer Meeting, 11-15 June 2000, Boston, Massachusetts

5. **Eastwick, C, Hibberd, ,. Simmons, K, Wang, Y, Care, I, Aroussi, A,** "Using CFD to improve aero-engine air/oil separator design", 2002,ASME, Pressure Vessels and Piping Division (Publication) PVP vol 448, pp215-220.
6. **Hossain, M, Wang, Y, Eastwick, CN, Simmons, K & Hibberd, S,** "Comparison Of Flow Characteristics For Two Aero-Engine Air/Oil Separators", 2000, NAFEMS Conference "Industrial CFD And The Move Towards Multiphase Analyses", 8 Nov 2000, Warwick University.
7. **Aroussi. A, Menacer M,** "Report on the Techspace Aero Tests", 2001, Internal Report, Brite Euram EU project INTRANS.
8. **Wittig S., Glahn A. and Himmelsbach J.** "Influence of high rotational speeds on heat transfer and oil film thickness in aero engine bearing chambers", 1993, ASME paper 93-GT-209.
9. **Wittig S., Glahn A. and Himmelsbach, J.** "Influence of high rotational speeds on heat transfer and oil film thickness in aero engine bearing chambers", 1994, Journal of Engineering for Gas Turbines and Power, Trans. ASME, **116**, pp.395-401.
10. **Glahn A., Kurreck M., Willmann M., and Wittig S.** "Feasibility study on oil droplet flow investigations inside aero engine bearing chambers - PDPA techniques in combination with numerical approaches", 1995a, ASME Paper (Conference code 43400), p.9.
11. **Glahn A. and Wittig S.** "Two-phase air/oil flow in aero engine bearing chambers - characterization of oil film flows", 1995b, ASME Paper (Conference code 43400), p.8.

12. **Daily, J.W. & Nece, R.E.,** " Chamber Dimension Effects on induced flow and frictional resistance of enclosed rotating disks", 1960, Journal of Basic Engineering, **82**, pp. 217 – 230.
13. **Michaelides, E.E.,** , Review – The transient equation of motion for particles, bubbles and droplets, 1997 Journal of Fluids Engineering, **119**, pp. 233-247.
14. **Farrall, M.**, "Numerical Modelling of Two-Phase Flow in a Simplified Bearing Chamber", 2000, PhD thesis, University of Nottingham.
15. Farrall, M, Simmons, K, Hibberd, S, Gorse, P, "A numerical model for oil film flow in an aero-engine bearing chamber and comparison with experimental data", 2004, ASME Turbo Expo 2004 paper GT2004-53698.
16. **Lage, J.L.,** "The fundamental theory of flow through porous media from Darcy to Turbulence", 1998, from Transport Phenomena in Porous Media, Elsevier Science Ltd., Ed. Ingham & Pop.
17. **Dunlop**, "Dunlop Equipment Retimet deoilers for aero-engines", 1997, Aircraft Eng. and Aerospace Tech., **69,** pp. 64-66.
18. **Phillips, A.G.** "Two-phase flow in rapidly rotating porous media", 2003, PhD thesis, University of Nottingham.
19. **Dunlop**, 1980, Retimet Data Sheet. Dunlop Equipment Ltd. England.
20. **CFX User Guide**, 1997, Release 4.2. AEA Technology, England.
21. **Launder, B.E. and Spalding, D.B.,** "The numerical computation of turbulent flows". 1974, Computational Methods in Applied Mechanical Engineering, **3,** pp. 269-289.
22. **Spalding, D.B.**, "A novel finite-difference formulation for differential expressions involving both first and second derivatives", 1972, International Journal of Numerical Methods in Engineering, **4**, pp.551-559.

23. **Van Doormal, J.P. and Raithby, G.D.,** "Enhancements of the SIMPLE method for predicting incompressible fluid flows", 1984, Numerical Heat Transfer, **7**, pp. 147-163.

24. **Lonsdale, R.D.,** "An algebraic multi-grid solver for the Navier stokes equation on unstructured meshes", 1993, International Journal of Numerical Methods in Heat and Fluid Flow, **3**, 1, pp. 3-14.

List of Captions

Study of aero-engine oil/air separators

C N Eastwick[1], K Simmons[1], Y Wang[2] & S Hibberd[1]

Figure 1

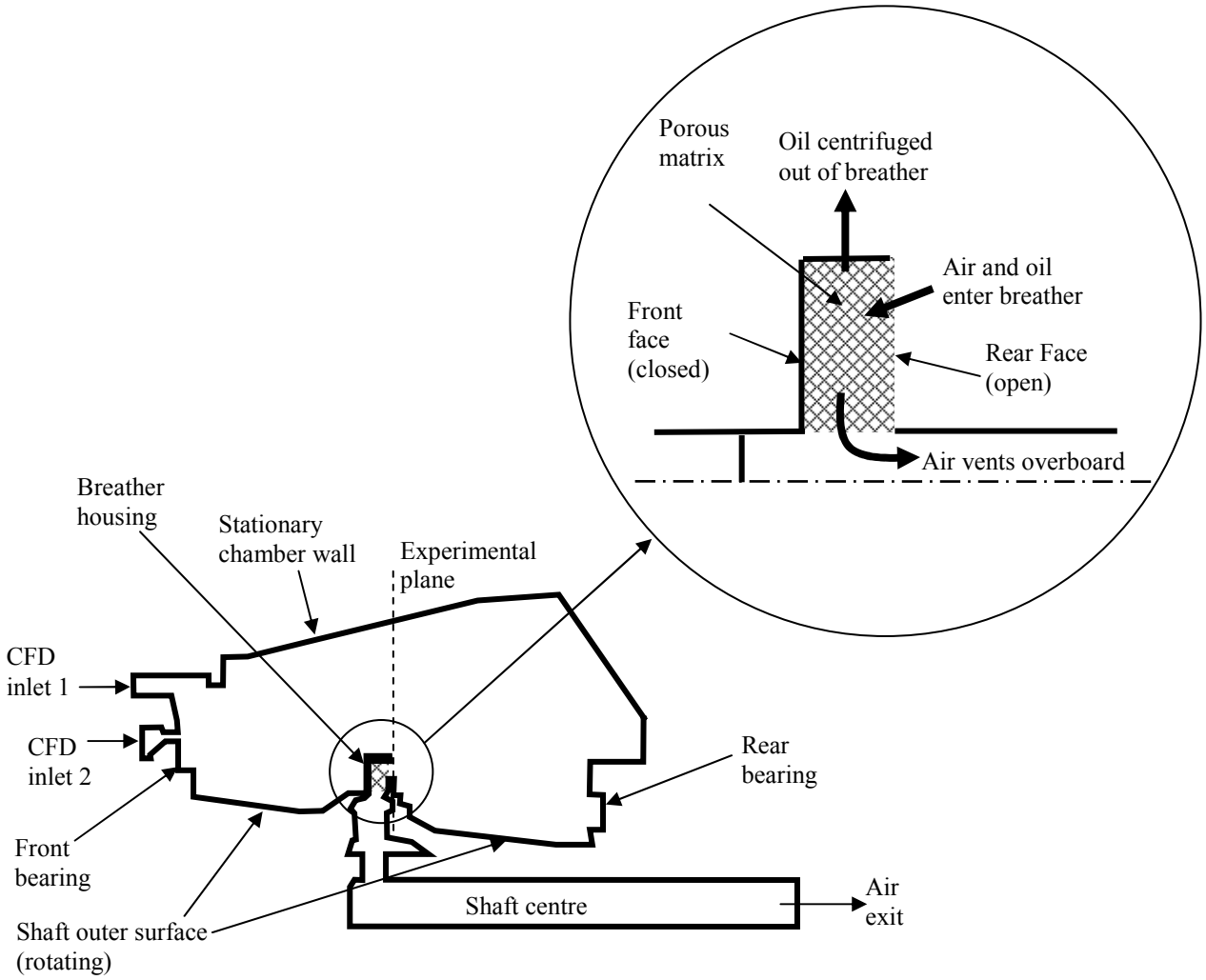

Study of aero-engine oil/air separators

C N Eastwick[1], K Simmons[1], Y Wang[2] & S Hibberd[1]

Figure 2

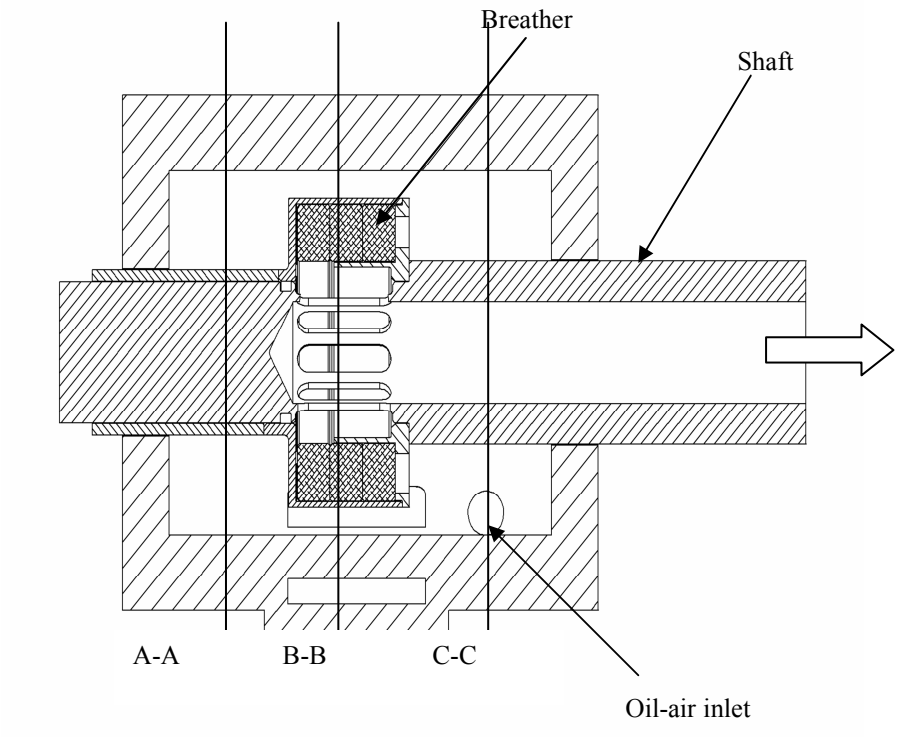

Study of aero-engine oil/air separators

C N Eastwick[1], K Simmons[1], Y Wang[2] & S Hibberd[1]

Figure 3

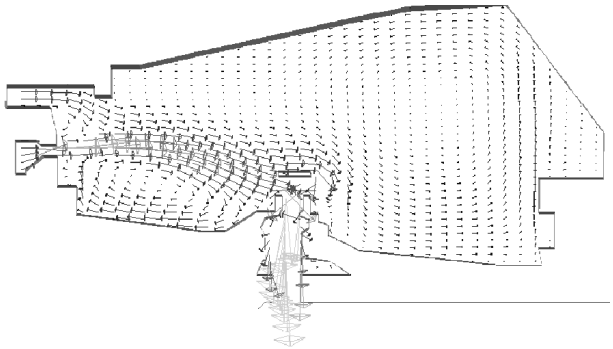

(a) Front and rear open case, 1100 rpm

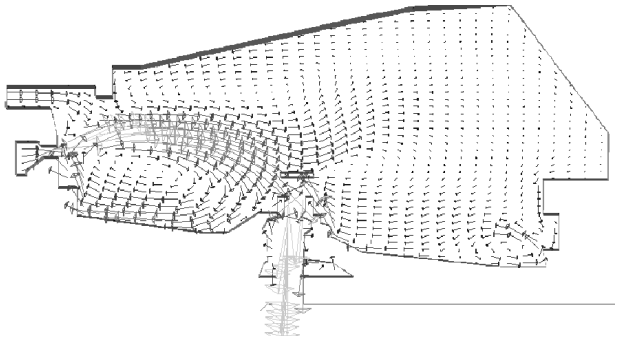

(a) Front and rear open case, 5000 rpm

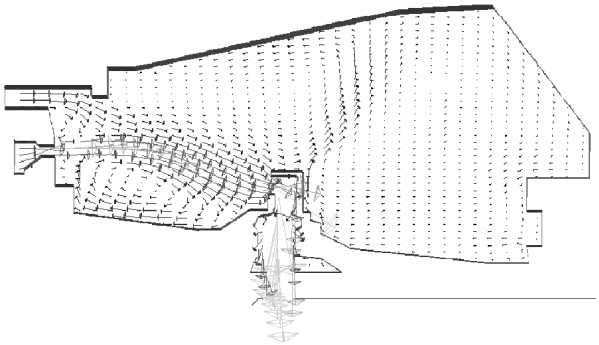

(c) Front open case, 1100 rpm

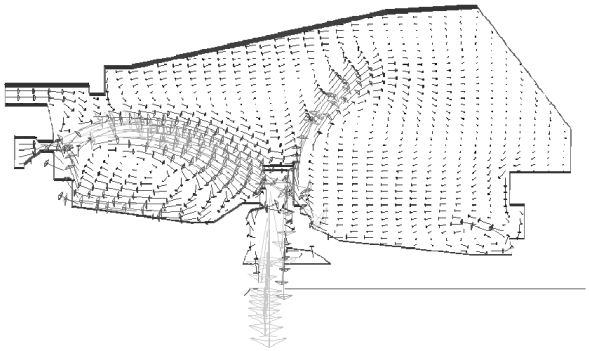

(d) Front open case, 5000 rpm

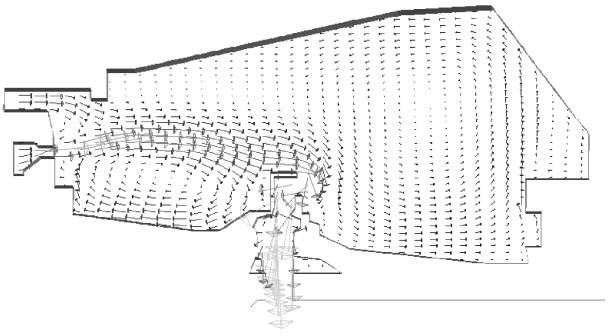

(e) Rear open case, 1100 rpm

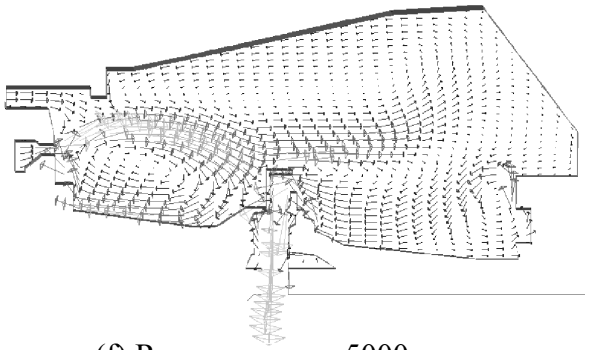

(f) Rear open case, 5000 rpm

Study of aero-engine oil/air separators

C N Eastwick[1], K Simmons[1], Y Wang[2] & S Hibberd[1]

Figure 4

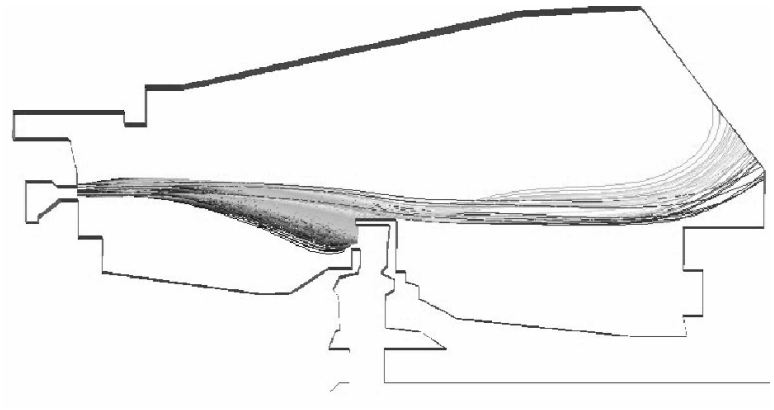

a) front open case, 1100 rpm

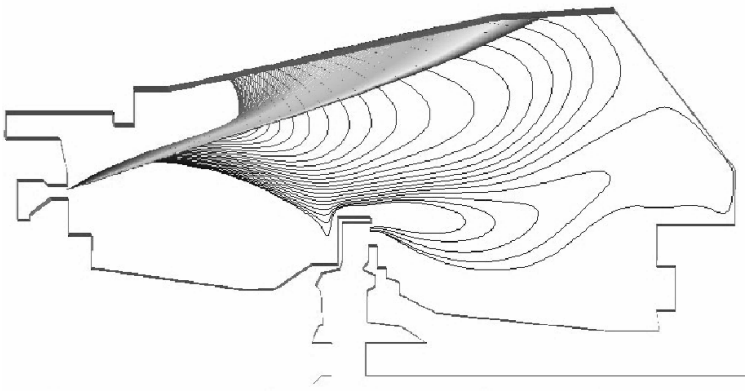

a) rear open case, 5000 rpm

Study of aero-engine oil/air separators

C N Eastwick[1], K Simmons[1], Y Wang[2] & S Hibberd[1]

Figure 5

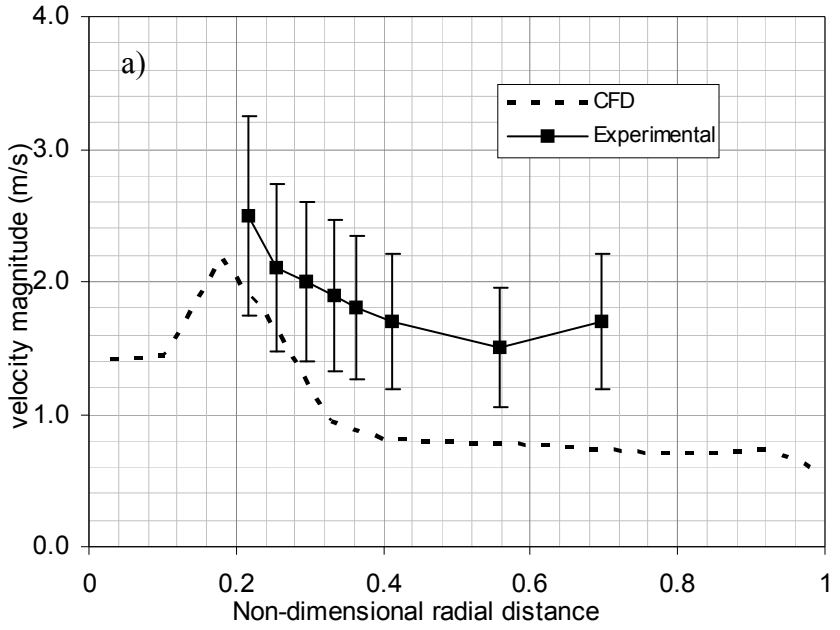

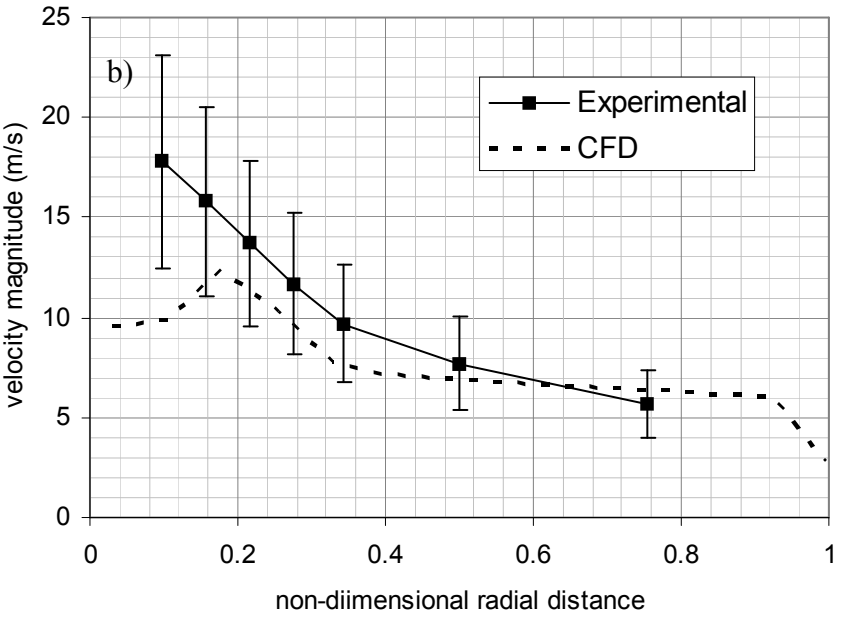

Study of aero-engine oil/air separators

C N Eastwick[1], K Simmons[1], Y Wang[2] & S Hibberd[1]

Figure 6

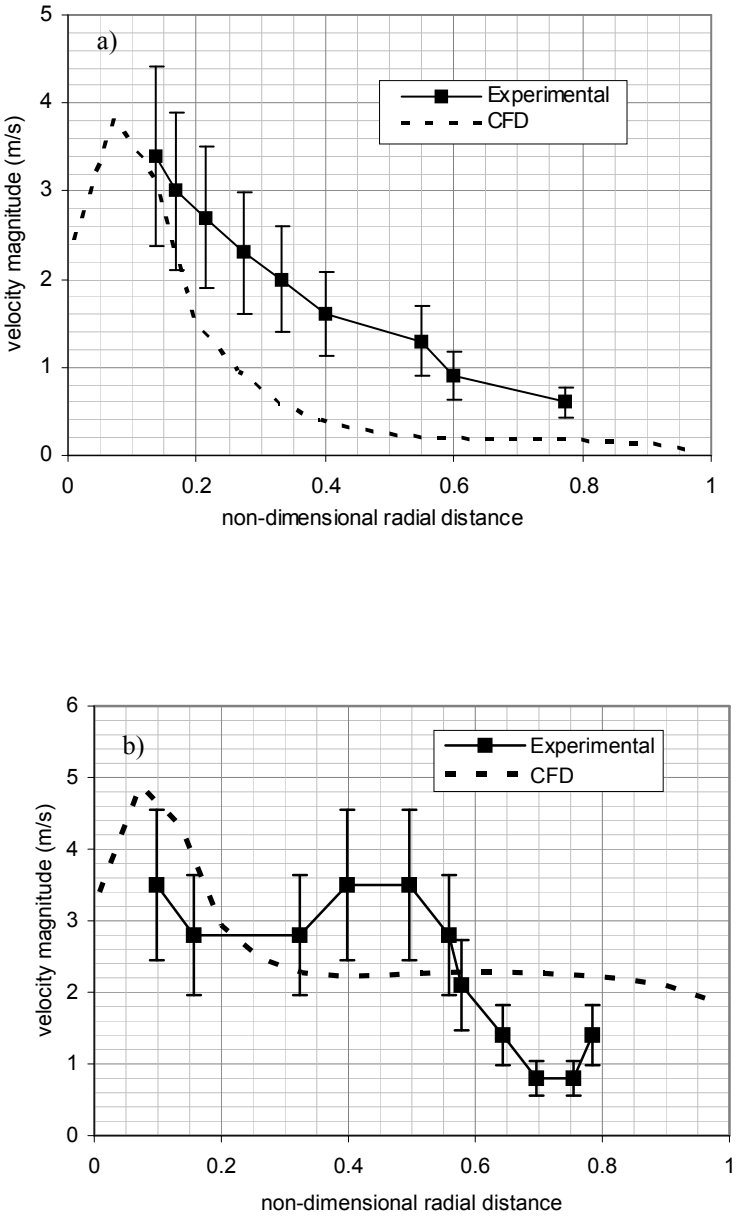

Study of aero-engine oil/air separators

C N Eastwick[1], K Simmons[1], Y Wang[2] & S Hibberd[1]

Figure 7

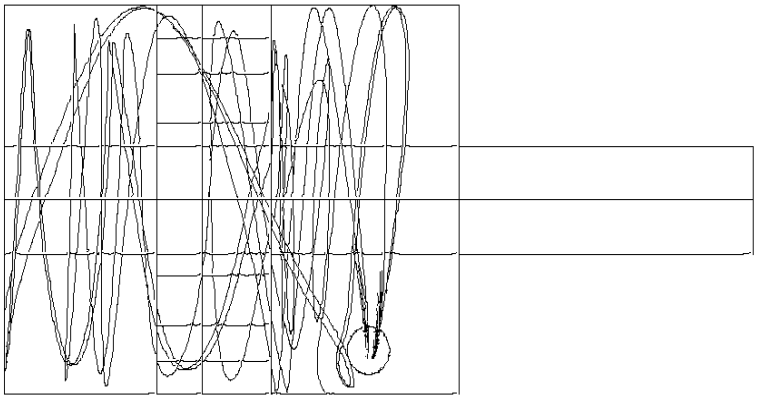

a) Single inlet

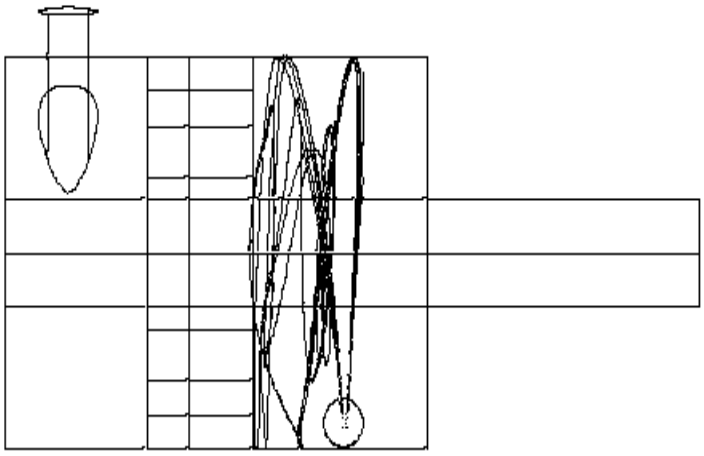

b) Two inlets

Study of aero-engine oil/air separators

C N Eastwick[1], K Simmons[1], Y Wang[2] & S Hibberd[1]

Figure 8

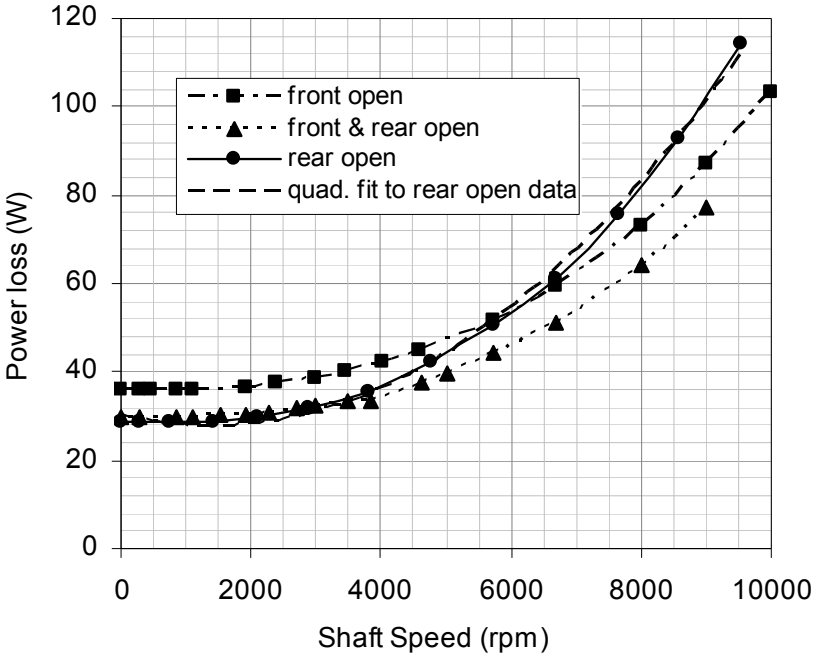

a) Internal design

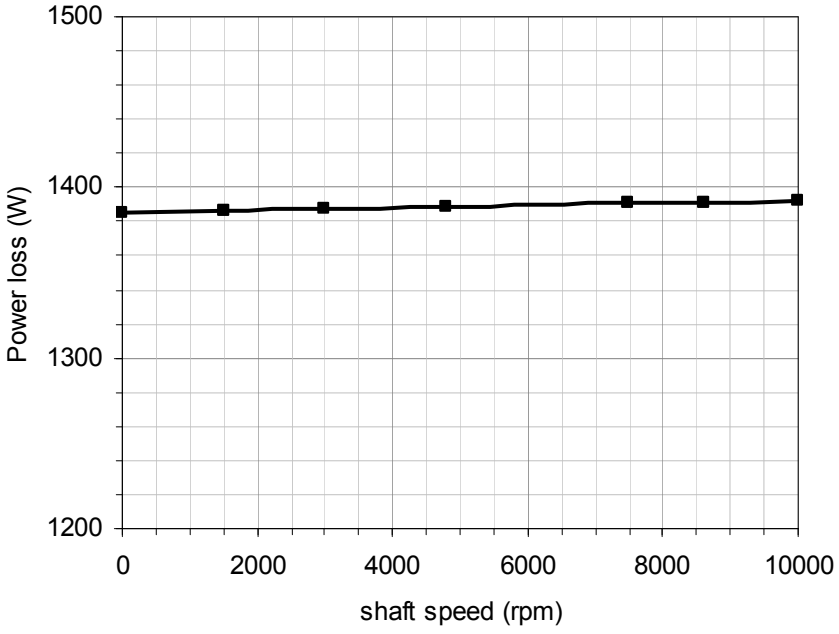

b) External design

Study of aero-engine oil/air separators

C N Eastwick[1], K Simmons[1], Y Wang[2] & S Hibberd[1]

Figure 9